2013 European Control Conference (ECC)
July 17-19, 2013, Zürich, Switzerland.

Dynamic Real-Time Optimization and Control of a Hybrid Energy System

M. Trifkovic* , W.A. Marvin*, M. Sheikhzadeh†, P. Daoutidis*
*Department of Chemical Engineering and Materials Science, University of Minnesota, Minneapolis, Minnesota
†Department of Instrumentation and Control, Lambton College, Sarnia, Canada

***Abstract*—A proactive energy management strategy for a stand-alone hybrid renewable energy system is presented. The study was motivated by the system built in Lambton College (Sarnia, Ontario, Canada) which includes photovoltaic arrays, wind turbine, battery, electrolyzers, hydrogen storage tanks, and fuel cells. The control architecture consists of two levels of hierarchy: (1) an optimal predictive scheduling at the supervisory level; (2) system unit control at the low level. A "day-ahead" approach is followed at the supervisory level and a bidirectional communication between the supervisory, proactive control, and the low level control layer. The proposed energy management strategy accounts for external (i.e. weather and demand) and internal disturbances.**

I. Introduction

Pressing environmental issues, security of energy supply sites, and nuclear power safety concerns drive research and development towards renewable energy sources (RES) worldwide. A key attribute of RES, such as wind and solar resources, is intermittency. RES are not dispatchable, they exhibit large fluctuations, and are uncertain. Consequently, only 3% of the total electricity is currently generated from non-hydro RES [1].

The intermittency of RES can be absorbed by the hybrid combination of different RES, and distributed resources such as energy storage, programmable loads and smart appliances [2]–[5]. The choice of different RES (e.g. wind and solar) as well as storage devices (hydrogen, compressed air, pumped hydroelectric systems, batteries, supercapacitors) depends on the location, the hybrid energy system's operational mode (stand-alone vs. grid-connected) and its size. In order to realize such a system's full benefit, resources have to be coordinated to efficiently and reliably provide services (e.g. power, hydrogen) in the face of uncertainty that arises from renewables and consumers [6], [7].

To address the issues associated with RES, there has been a growing interest in the development of energy management algorithms for islanded and grid-connected hybrid energy systems. The problem is that of finding the optimal (or near optimal) unit commitment and dispatch of renewable energy so that certain objectives are achieved. A commonly pursued objective for a stand-alone mode of operation is to economically supply a local load, whereas under a grid-connected mode the maximization of profit is typically sought [8]. Additional objectives such as the minimization of greenhouse gas emissions by applying heuristic and multi-objective optimization techniques have been reported [9]. The majority of existing studies have reported algorithms that are reactive in nature, i.e. acting in response to power imbalances between generation and demand [6], [10], [11]. Recent research has sought to encorporate predictions to deliver proactive unit commitment. Significant cost savings have been demonstrated when load predictions and weather/ambient condition forecasts are included [12], [13]. Similarly, grid-connected configurations have been shown to benefit from proactive unit commitment that includes electricity price predictions [14]. However, only a few of these, either reactive or proactive, algorithms have been implemented in real time due to the high capital cost associated with renewable energy systems [15], [16].

Our previous study concerned a hybrid system built in Sarnia, Ontario, Canada and focused on the development of rigorous process models and local controllers for each system's unit [17], [18]. We also developed a power management structure, which consisted of two layers: supervisory and low-level control. Although the supervisory controller offered fast execution, it was reactive in nature as it addressed only power imbalances between generation and demand. Moreover, the strategy did not have the capability of handling large-scale hybrid systems which may consist of multiple units. In this study we use the previously developed computational platform (the dynamic model and local controllers) and employ a dynamic real-time optimization (D-RTO) layer as the supervisory controller. The aim is to exploit the forecasted exogenous disturbance trends in an optimal way, reject internal (to the system) disturbances, enable increased flexibility through modular design and increase the units' lifetime by minimizing the number of startups and shutdowns. A key feature of the proposed strategy is a bidirectional communication between the D-RTO and low level control layers to account for internal as well as exogenous disturbances. A case study, demonstrating the effectiveness of the proposed control structure, is presented.

II. Control Architecture

The hybrid energy system of interest in this study consists of the following subsystems: wind and solar energy conversion units, three electrolyzers, low and high pressure hydrogen tanks, hydrogen compressor, two fuel cells and a battery subsystem. The generated power from the RES can be used directly to meet the load demand, to generate hydrogen (through the electrolyzers), or to charge the battery. Hydrogen

generated by the electrolyzers is stored in the low pressure hydrogen tank, which then can be used either to run the fuel cells or be compressed and sent to the high pressure tank. On the other hand, when power generated from the RES is not sufficient to meet the load demand, the power deficit can be corrected by either discharging the battery or activating the FC stacks which consume previously stored hydrogen in the low or high pressure tank and convert it to electricity. The fuel cell activation occurs only if there is a sufficient supply of hydrogen in the storage tank. The overall system and control architecture are shown in Fig. 1.

Over a time horizon t^h, an optimal plan for the controllable units is calculated by the D-RTO layer and sent to the local controllers, which enforce the optimal profiles to the respective units. The optimal profile consists of the unit commitments (binary controls) and its corresponding power setpoints (continuous controls) according to the expected RES, demand profiles and storage status for the next t^h. The updated demand and RES power profiles as well as the current states of the system are sent from the low-level back to the supervisory controller at each optimization interval, Δt_{opt}. Thus, the optimization problem is solved in a closed-loop manner by updating the current states and forecasts on a moving horizon window. The units are operated always at their rated power to ensure that the system achieves its maximum efficiency. The supervisory controller development was carried out in GAMS while the local controllers and the dynamic model were developed in MATLAB. The connection between the two layers was established using the MATLAB/GAMS interface [19]. The optimization layer uses a discretized model, with a relatively large time discretization step to minimize computational demand. Any mismatch with the real-time simulations of the overall process is dealt with by the local controller and a dynamic storage system (batteries) which serves to buffer power. Although its setpoint is determined by the supervisory D-RTO layer, it is further refined and adjusted on a smaller sampling interval according to the balance between generated and used power.

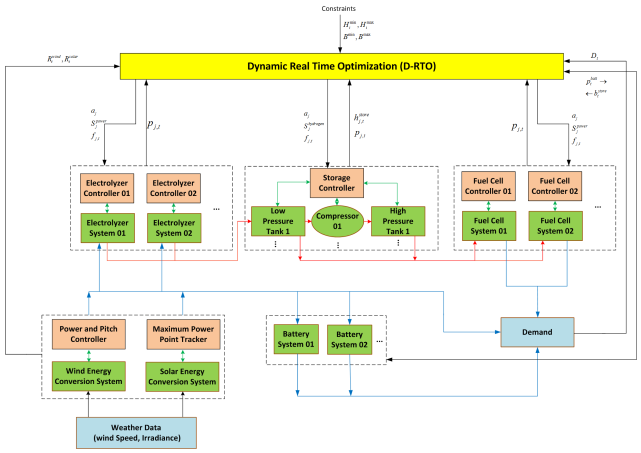

Fig. 1. Control Architecture

For the case study, the bidirectional update interval between the supervisory and low level control layer, (Δt_{opt}), is established on as 1 hr, while the moving horizon, t^h, is set to 24 hr. The battery's setpoint is determined on a one-second basis. Battery charging/dischanging, p_t^{batt} is calculated through the balance of the utilized wind u_t^{wind} and solar energy u_t^{solar}, the electrolyzer power consumption, fuel cell power generation and power demand D_t according to the following equation:

$$p_t^{\text{batt}} = u_t^{\text{wind}} + u_t^{\text{solar}} - \sum_{j \in \mathbf{J}^e} p_{j,t} + \sum_{j \in \mathbf{J}^f} p_{j,t} - D_t \quad (1)$$

The high resolution update of the battery setpoint allows for quickly addressing any internal disturbances, arising from a malfunction of any of the system units, as well as the model mismatch between the supervisory and low-level control layer. Similarly, the low pressure hydrogen tank setpoint determined by the supervisory layer can be overwritten in the event that the hydrogen level in the tank is not sufficient to meet the demand. In that case, a remainder is taken from the high pressure hydrogen tank.

The hierarchical nature of the proposed power management strategies allows to account for external and internal disturbances, while minimizing communication between the different layers and computation time required for planning.

III. D-RTO Formulation

Our real-time optimization layer solves a dynamic optimization problem from the current time t^0 over the time horizon $\tau \in \left[t^0, t^0 + t^h\right]$, and has the general form:

$$\min_{u(\tau)} \quad \int_{t^0}^{t^0+t^h} \varphi\left(z(\tau), u(\tau), \chi(\tau)\right) d\tau \quad (2a)$$

$$\text{subject to } \frac{dz}{d\tau} = \mathbf{f}\left(z(\tau), u(\tau), \chi(\tau)\right) \quad (2b)$$

$$0 = \mathbf{g}\left(z(\tau), u(\tau), \chi(\tau)\right) \quad (2c)$$

$$0 \geq \mathbf{h}\left(z(\tau), u(\tau), \chi(\tau)\right) \quad (2d)$$

$$z(t^0) = z^0, \ \forall \tau \in \left[t^0, t^0 + t^h\right] \quad (2e)$$

where $z(\tau)$ are the state variables, $u(\tau)$ are the controlled variables and $\chi(\tau)$ are the disturbances. The dynamic model of the system is expressed in (2b,c) with operating constraints in (2d), and initial states in (2e).

We transform (2) into the following linear/nonlinear program (depending on the functional form of $\mathbf{f}$, $\mathbf{g}$ and $\mathbf{h}$) by discretizing the time horizon into time periods $t \in \{1, \ldots, T\}$ with uniform duration $\Delta t = t^h/T$:

$$\min_{u(t)} \quad \Delta t \cdot \sum_t \varphi\left(z(t), u(t), \chi(t)\right) \quad (3a)$$

$$\text{subject to } z(t) = \Delta t \cdot \mathbf{f}\left(z(t), u(t), \chi(t)\right) + z(t-1) \quad (3b)$$

$$0 = \mathbf{g}\left(z(t), u(t), \chi(t)\right) \quad (3c)$$

$$0 \geq \mathbf{h}\left(z(t), u(t), \chi(t)\right) \quad (3d)$$

$$z(0) = z^0, \ \forall t \in \{1, \ldots, T\} \quad (3e)$$

The dynamic model of our hybrid energy system arrises from mass and energy conservation equations, which determine the trajectory of state variables (i.e. storage level for hydrogen and energy) as a function of the controlled

variables (e.g. wind and solar utilization, power and hydrogen usage/generation for each unit) and the disturbances (e.g. wind and solar availability, and energy demand). We consider a set of process units $\mathbf{J}$ indexed by j, which includes subsets for water electrolyzers $\mathbf{J}^e$, hydrogen fuel cells $\mathbf{J}^f$ and gas compressors $\mathbf{J}^c$. A set of tanks for hydrogen storage $\mathbf{I}$ indexed by i includes subsets for low pressure $\mathbf{I}^l$ and high pressure $\mathbf{I}^h$.

A. Objective function

Multiple objective functions are of interest in the context of the energy system optimization in hybrid energy systems. In this particular case we choose to maximize the utilization of renewable resources (u_t^{wind} and u_t^{solar}), and the amount of stored hydrogen ($h_{i,t}^{\text{store}}$), and to minimize the number of startups and shutdowns ($y_{j,t}$) of all of the system's units:

$$\max_{\substack{h_{i,t}^{\text{store}}, y_{j,t}, \\ u_t^{\text{wind}}, u_t^{\text{solar}}}} \sum_{\text{j}\in\mathbf{J}} \sum_{\text{i}\in\mathbf{I}} \left(C^{\text{w}} u_t^{\text{wind}} + C^{\text{s}} u_t^{\text{solar}} + C^{\text{h}} h_{i,t}^{\text{store}} - C^{\text{y}} y_{j,t} \right) \tag{4}$$

$C^{\text{w}}, C^{\text{s}}, C^{\text{h}}, C^{\text{y}}$ are the weight factors associated with the objectives addressed in this optimization formulation.

B. Constraints

Power demand D_t is satisfied in each time period through a balance of utilized wind u_t^{wind} and solar u_t^{solar} resources, electrolyzer power consumption, fuel cell power generation and battery charging/dischanging p_t^{batt}:

$$u_t^{\text{wind}} + u_t^{\text{solar}} - \sum_{j\in\mathbf{J}^e} p_{j,t} + \sum_{j\in\mathbf{J}^f} p_{j,t} - p_t^{\text{batt}} = D_t, \ \forall t \tag{5}$$

Utilized wind and solar resources cannot exceed the amounts harvestable:

$$u_t^{\text{wind}} \le R_t^{\text{wind}}, \ \forall t \tag{6}$$

$$u_t^{\text{solar}} \le R_t^{\text{solar}}, \ \forall t \tag{7}$$

Each unit can be on for some fraction $f_{j,t}$ of each time period. If unit j is on at any point during t, then the binary variable $a_{j,t} = 1$:

$$f_j^{\min} \cdot a_{j,t} \le f_{j,t} \le a_{j,t}, \ \forall j,t \tag{8}$$

$$0 \le f_{j,t} \le 1, \ \forall j,t \tag{9}$$

$$a_{j,t} \in [0,1], \ \forall j,t \tag{10}$$

where $f_j^{\min}$ is the minimum time that unit j can be operated.

The binary variable $y_{j,t} = 1$ if unit j turns from off to on during time period t. This is accomplished with the constraints:

$$y_{j,t} \ge a_{j,t} - a_{j,t-1}, \ \forall j,t \tag{11}$$

$$y_{j,t} \le a_{j,t}, \ \forall j,t \tag{12}$$

$$a_{j,0} = a_j^0, \ \forall j \tag{13}$$

where a_j^0 is the initial state of each unit.

If a unit was previously operating and continues to be on into the next time period, two scenarios can occur. Either the unit is shut down briefly (i.e. $f_{j,t} < 1$, $y_{j,t} = 1$) or the unit operates for the whole time period (i.e. $f_{j,t} = 1$, $y_{j,t} = 0$). This is enforced by:

$$f_{j,t} \ge a_{j,t-1} + a_{j,t} + a_{j,t+1} - 2 - y_{j,t}, \ \forall j,t \tag{14}$$

Once turned on, the unit quickly reaches power setpoint S_j^{power} and hydrogen setpoint S_j^{hydrogen}. The amount of generated/consumed power and hydrogen during the time period is then:

$$p_{j,t} = S_j^{\text{power}} \cdot f_{j,t} \tag{15}$$

$$h_{j,t}^{\text{gen}} = S_j^{\text{hydrogen}} \cdot f_{j,t} \tag{16}$$

Hydrogen produced by the electrolyzers is sent to low pressure tanks. Low pressure hydrogen can then be compressed and sent to high pressure tanks, or sent to fuel cells. Hydrogen in high pressure tanks can also be sent to fuel cells.

$$h_{j,t} = \sum_{i\in\mathbf{I}^l} h_{i,j,t}^{\text{gen}}, \ \forall j \in \mathbf{J}^e, t \tag{17}$$

$$h_{i,t}^{\text{store}} = h_{i,t-1}^{\text{store}} + \sum_{j\in\mathbf{J}^e} h_{i,j,t}^{\text{gen}} - \sum_{i'\in\mathbf{I}^h, j\in\mathbf{J}^c} h_{i,i',j,t}^{\text{comp}} - \sum_{j\in\mathbf{J}^f} h_{i,j,t}^{\text{cons}}, \ \forall i \in \mathbf{I}^l, t \tag{18}$$

$$h_{j,t} = \sum_{i\in\mathbf{I}^l, i'\in\mathbf{I}^h} h_{i,i',j,t}^{\text{comp}}, \ \forall j \in \mathbf{J}^c, t \tag{19}$$

$$h_{i,t}^{\text{store}} = h_{i,t-1}^{\text{store}} + \sum_{i\in\mathbf{I}^l, j\in\mathbf{J}^c} h_{i,i',j,t}^{\text{comp}} - \sum_{j\in\mathbf{J}^f} h_{i,j,t}^{\text{cons}}, \ \forall i \in \mathbf{I}^h, t \tag{20}$$

$$h_{j,t} = \sum_{i} h_{i,j,t}^{\text{cons}}, \ \forall j \in \mathbf{J}^f, t \tag{21}$$

Power can be stored or discharged from the battery as needed:

$$b_t^{\text{store}} = b_{t-1}^{\text{store}} + p_t^{\text{batt}}, \ \forall t \tag{22}$$

Hydrogen storage and battery storage are bounded and have initial conditions:

$$H_i^{\min} \le h_{i,t}^{\text{store}} \le H_i^{\max}, \ \forall i,t \tag{23}$$

$$B^{\min} \le b_t^{\text{store}} \le B^{\max}, \ \forall t \tag{24}$$

$$h_{i,0}^{\text{store}} = H_i^0, \ \forall i \tag{25}$$

$$b_0^{\text{store}} = B^0 \tag{26}$$

IV. Case Study

The hybrid system units and their corresponding power ratings are summarized in Table I. The presented simulation results are based on average weather data (wind velocity and solar irradiance) for the month of July in the Sarnia, Ontario region, and a typical load demand (D_t) of the hybrid system (see Fig. 2).

We present the system's performance for 34 hours. At each optimization interval Δt_{opt}, D-RTO estimated the optimal setpoint trajectories for the controlled variables (u) and

TABLE I
HYBRID ENERGY SYSTEM DESIGN

Unit Name	Rating Power (kW)	Number of Units
Wind System	8	1
Solar System	2.2	1
Electrolyzer 1	2.3	1
Electrolyzer 2	1.1	2
Fuel Cell	1.1	2
Compressor	2.3	1
Battery	2	1

passed them to the low level controllers. The sampling time for the local controllers was set to one second. The estimated controlled variables by the D-RTO layer were the unit commitments for the electrolyzers, fuel cells, and compressor ($a_{j,t}$), the fraction of the time period that units were on ($f_{j,t}$), the unit power setpoints ($S_{j,t}$), the battery charge and discharge power (p_t^{batt}) as well as the output hydrogen flow rates from the low and high pressure hydrogen tanks ($h_{i,j,t}^{\text{cons}}$). Although, the D-RTO calculated the "day-ahead" optimal trajectories, only the interval ($t^0+\Delta t_{opt}$) was enforced before the next optimization interval. The current and forecasted demand (D_t) and the RES power profiles (R_t^{wind} and R_t^{solar}), as well as the amount of stored hydrogen in tanks ($h_{i,j,t}^{\text{store}}$), battery charge status (b_t^{store}) and the unit status (binaries) were sent from the low level control layer back to the D-RTO at each Δt_{opt} for the estimation over the next t^h horizon. Note that the hierarchical scheme introduced in this article relies on credible forecasts. Without this assumption the proactive actions cannot be guaranteed to be effective and the system performance would degrade.

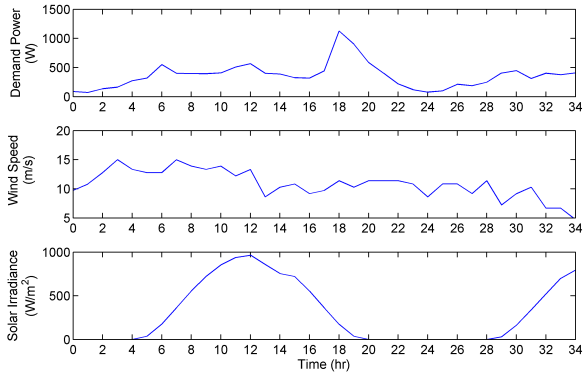

Fig. 2. Average Demand, wind velocity and solar irradiance data

To illustrate the proactiveness and robustness of the control strategy, we present the optimal setpoint trajectories for the selected units after the first, fifth and ninth optimization interval ($Opt_{1,5,10}$) in Fig. 3. The initial plan based on the daily optimization (shown by the dashed lines) was altered in the future optimization intervals as a result of the feedback from the low level control layer. The updated states were used as initial conditions for the calculation of the next optimal trajectory, and the future weather and demand trends were revised, which consequently altered the optimal plan for the next 24 hrs. For example, in the Opt_5 scenario, as a result of the decreased demand at 25hr, the high capacity electrolyzer (ELE_1) was activated. The Opt_{10} scenario (shown by the solid lines) started from the rated power for the electrolyzers and fuel cell. This indicates that these units were on in the previous interval (Opt_9), and their previous state was used as the initial condition in the current (Opt_{10}) optimization interval. Also, Opt_1 and Opt_5 did not predict the activation of the fuel cells within their horizon, however, at Opt_{10} the D-RTO estimated the fuel cell activation once.

The continuous update of the system's states as well as the change in weather and demand trends affected the optimization solutions. It is also important to note that due to the fractional variables in the optimization formulation, the units (e.g. the fuel cell, compressor) could be on for only a fraction of the optimization interval , which allowed us to have a relatively infrequent calculation of optimal trajectories (set to 1 hr).

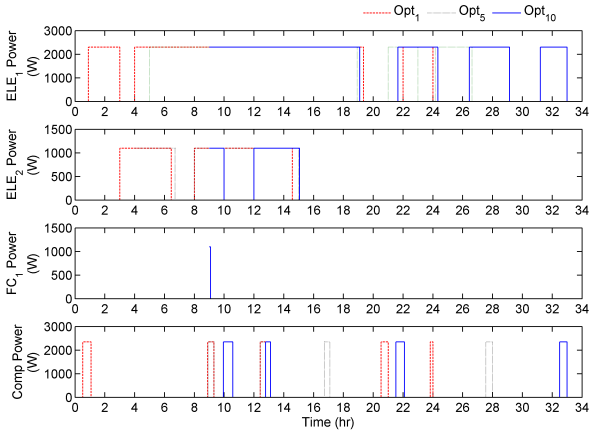

Fig. 3. Estimated power setpoint for each subsystem calculated by D-RTO at t=0 (Opt_1), t=4hr (Opt_5) and t=9hr (Opt_{10})

Fig. 4 depicts the realized dynamics of the system to illustrate the model dynamics as well as the control action at the low level control layer. The figure inset shows in detail the real-time setpoint tracking for the electrolyzer.

Fig. 5 shows the battery dynamics and its variation from the setpoints determined by the D-RTO layer. As mentioned previously, the battery serves as a buffer at the low level control layer. Although the realized battery's state of charge (SOC) followed the overall trend determined by the D-RTO, it differed from it within the one-hour optimization interval.

The low and high pressure hydrogen tanks act as a short term and long term hydrogen storage, respectively. The tanks fill percentages are presented in Fig. 6. From the depicted profiles, it can be seen that the low pressure tank served as the main supply of hydrogen for the fuel cells due to the high RES availability during this period. Also, when it reached its maximum capacity, its content was sent to the compressor and subsequently to the high pressure tank. The tanks' output flowrates (S_j^{hydrogen}) were estimated by the D-RTO algorithm. During the presented 34hr period, hydrogen from the high

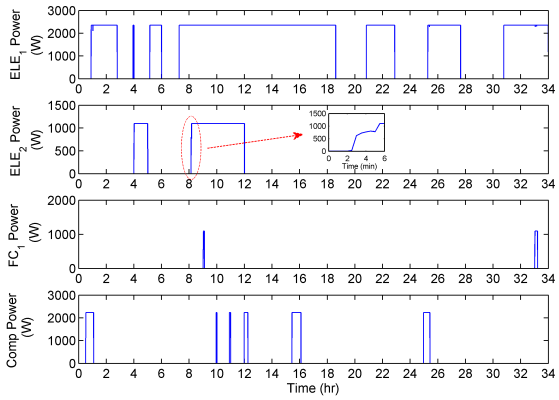

Fig. 4. Realized power for hybrid energy system components

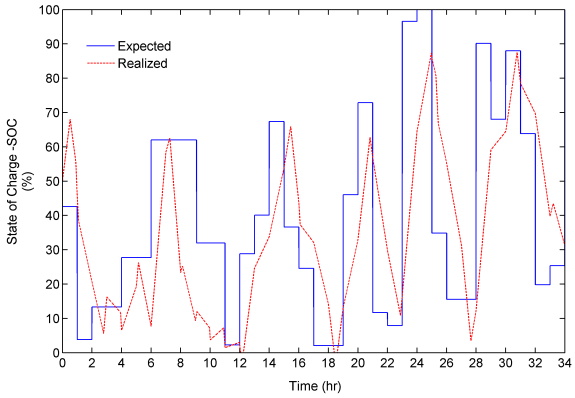

Fig. 5. Expected and realized battery state of charge

pressure tank was not used to supply the fuel cels, which was expected considering that there was a cost associated with storing hydrogen in the high pressure tank (the compressor had to be activated and power used). Note that the compressor and the high pressure tank in this system are purposely oversized, as the strategic plan of Lambton College is to expand the hybrid energy system and use generated hydrogen for other purposes too. Consequently, a large amount of power was needed to run the compressor, which was the main reason for the short time intervals that the compressor was on. The flowrates from the low and high pressure hydrogen tanks could be overwritten at the low level control layer in the event that pressure in the tank was not sufficient to meet the fuel cells' demand. The low-level flow controller received the D-RTO's flowrate setpoints as well as the updated tank content on a one-second basis. If the amount of hydrogen in the tanks was sufficient to meet the fuel cells' demand, the calculated flowrates were enforced. Otherwise, the flowrate controller rejected the D-RTO decision and determined the flowrates according to the tanks' current status. A priority was still given to the low pressure tank, and the remainder was fulfilled with hydrogen from the high pressure tank. This change in the tank storage level was communicated to the D-RTO layer in the next optimization interval.

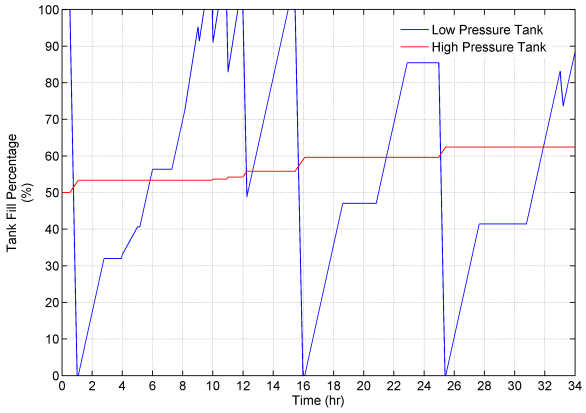

Fig. 6. Low and high pressure Hydrogen tank fill percentage

Fig. 7 depicts the realized power trends of all the system's components, and illustrates the overall performance of the hybrid energy system. Each component except the battery (which serves as a power buffer) is shown by the stacked area. The power generators are stacked above and power users below zero. The difference between the two should equate to the battery's power (shown by the solid line). The graph shows that the RES were utilized efficiently through either meeting the demand or storing hydrogen. The battery's dynamic also illustrates that it successfully provided the power balance between the power generators and power users in the system.

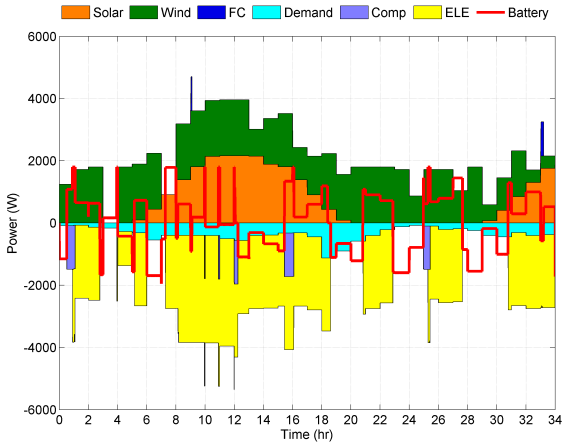

Fig. 7. Power balance of the hybrid energy system

V. Conclusions

The concept of a hybrid energy system which corresponds to the coordinated operation of load, renewable power generators and energy storage systems, is quite appealing due to its flexibility, controllability and energy management capabilities. In order to provide uninterrupted power supply, such a system has to economically meet the demand on an instantaneous basis. This paper has proposed a proactive hierarchical energy management strategy for the hybrid

energy system built in Lambton College, Sarnia, Canada. Although the study was motivated by this particular system, the proposed control strategy is applicable for optimal operation of future buildings capable of accommodating multiple units in standalone operation. The proposed strategy consists of long term resource scheduling by the dynamic real-time optimization (D-RTO) supervisory control layer and fast response to any unforeseen internal or external disturbance (demand or supply). The optimization formulation estimated the activating of the system's units for a fraction of the optimization interval, which consequently decreased the number of required optimizations. The feedback from the low to the D-RTO control layer allowed for incorporation of changes in the system states as well as any internal disturbances arising from a malfunction of system units. At the low level control layer, the fast dynamic energy storage served to buffer power and respond to the fast dynamic changes in the system. The performance of the control strategy was demonstrated through a case study with hydrogen and battery as storage systems. The D-RTO layer added a proactive feature to the overall control architecture with a high level of flexibility to integrate various operational, economical and safety objectives.

ACKNOWLEDGMENT

The authors would like to thank BlueWater Power Inc. for partial financial support and valuable suggestions, as well as the RECSR team at Lambton College. Partial financial support from the University of Minnesota's Institute on the Environment (IREE) project RL-0010-13 is also acknowledged.

REFERENCES

[1] Annual energy outlook 2011, tech. rep., U.S. Energy Information Administration, 2011.

[2] R. Karki, R. Billinton, "Reliability/Cost Implications of PV and Wind Energy Utilization in Small Isolated Power Systems," IEEE Trans. Energy Conver., vol. 16, no. 4, pp. 368-373, 2001.

[3] M. Santarelli, M. Cali, S. Macagno, " Design and Analysis of Stand-Alone Hydrogen Energy Systems with Different Renewable Sources," Intern. J. of Hydrogen Energy, vol. 29, no. 15, pp. 1571-1586, 2004.

[4] H. Yang, L. Lu, W. Zhou, "A Novel Optimization Sizing Model for Hybrid Solar-Wind Power Generation System" Solar Energy, vol. 81, no. 1, pp. 76-84, 2007.

[5] G. Giannakoudis, A. I. Papadopoulos, P. Seferlis, S. Voutetakis, "Optimum Design and Operation Under Uncertainty of Power Systems Using Renewable Energy Sources and Hydrogen Storage," International J. of Hydrogen Energy, vol. 35, no. 3, pp. 872-891, 2010.

[6] F. Valenciaga, P.F. Puleston, "Supervisory Control for a Stand-Alone Hybrid Generation System Using Wind and Photovoltaic Energy" IEEE Trans. Energy Conver., vol. 20, no. 2, pp. 398-405, 2005.

[7] J. L. Bernal-Agustn, R. Dufo-Lpez, "Simulation and optimization of stand-alone hybrid renewable energy systems," Renewable and Sustainable Energy Reviews, vol. 13, no. 8, pp.2111-2118, 2009.

[8] E. Alvarez, A. C. Lopez, J. Gomez-Aleixandre, N. de Abajo, On-line minimization of running costs, greenhouse gas emissions and the impact of distributed generation using microgrids on the electrical system, in Proc. IEEE PES/IAS Conference on Sustainable Alternative Energy (SAE), 2009, pp. 1-10.

[9] C. M. Colson, M. H. Nehrir, and S. A. Pourmousavi, Towards real-time microgrid power management using computational intelligence methods, in Proc. IEEE-PES General Meeting, Jul. 2010, pp. 1-8.

[10] C. Wang, M. H. Nehrir, "Power Management of a Stand-Alone Wind/Photovoltaic/Fuel-Cell Energy System," IEEE Trans. Energy Conver., vol. 23, no. 3, pp. 957-967, 2008.

[11] D. Ipsakis, S. Voutetakis, P. Seferlis, F. Stergiopoulos, C. Elmasides, "Power Management Strategies for a Stand-Alone Power system Using Renewable Energy Sources and Hydrogen Storage," International J. of Hydrogen Energy, vol. 35, no. 5, pp. 7081-7095, 2009.

[12] V. M. Zavala, E. M. Constantinescu, T. Krause, and M. Anitescu, On-Line Economic Optimization of Energy Systems Using Weather Forecast Information, Journal of Process Control, vol. 19, no.10, pp. 1725-1736, 2009.

[13] E. M. Constantinescu, V. M. Zavala, M. Rocklin, S. Lee, and M. Anitescu, A Computational Framework for Uncertainty Quantification and Stochastic Optimization in Unit Commitment with Wind Power Generation, IEEE Transactions on Power Systems, vol. 26, no.1, pp. 431-441, 2010.

[14] W. Qi, J. Liu, X. Chen, P. D. Christofides, "Supervisory Predictive Control of Stand-Alone Wind/Solar Energy Generation Systems," IEEE Trans. Control Systems Technology, vol. 19, no. 1, pp. 199-207, 2011.

[15] P. Hollmuller, J-M. Joubert, B. Lachal, K. Yvon, "Evaluation of a 5 kW Photovoltaic Hydrogen Production and Storage Installation for a Residential Home in Switzerland" International J. of Hydrogen Energy, vol. 25, no. 1, pp. 97-109, 2000.

[16] Ø. Ulleberg, T. Nakken, A. Eté, "The Wind/Hydrogen Demonstration System at Utsira in Norway: Evaluation of System Performance Using Operational Data and Updated Hydrogen Energy System Modeling Tools," International J. of Hydrogen Energy, vol. 35, no. 3, pp. 1841-1852, 2010.

[17] M. Trifkovic, M. Sheikhzadeh, K. Nigim, and P. Daoutidis, Modeling and Control of a Renewable Hybrid Energy System with Hydrogen Storage, submitted to IEEE Transactions on Control Systems Technology, 2012.

[18] M. Trifkovic, M. Sheikhzadeh, K. Nigim, and P. Daoutidis, Hierarchical Control of a Renewable Hybrid Energy System, In Proc. 51st IEEE Conference on Decision and Control , Maui, Hawaii, USA, 2012.

[19] M. C. Ferris, R. Jain, S. Dirkse, *GDXMRW: Interfacing GAMS and MATLAB*. Available: http://www.gams.com/dd/docs/tools/gdxmrw.pdf, 2011.